Engineering Science and Technology, an International Journal 19 (2016) 171–177

HOSTED BY

Contents lists available at ScienceDirect

Engineering Science and Technology, an International Journal

journal homepage: http://www.elsevier.com/locate/jestch

Full Length Article

A novel design for low insertion loss, multi-band RF-MEMS switch with low pull-in voltage

Mahesh Angira [a,*], KamalJit Rangra [b]

[a] EEE Department, BITS PILANI, Pilani, Rajasthan 333031, India
[b] SNT Group, CEERI, Pilani, Rajasthan 333031, India

ARTICLE INFO

Article history:
Received 31 December 2014
Received in revised form
18 June 2015
Accepted 3 July 2015
Available online 20 August 2015

Keywords:
Capacitive switch
Inductive tuning
Insertion loss
Multi-band
RF-MEMS

ABSTRACT

This paper presents a new type of capacitive shunt RF-MEMS switch. In the proposed design, float metal concept is utilized to reduce the RF overlap area between the movable structure and central conductor of CPW for improving the insertion loss of the device. This has been achieved without affecting the down-state response. Further, float metal also makes the down-state behavior predictable in terms of resonant frequency. For reducing the pull-in voltage, the switch is implemented with cantilever type of structure on either side of the transmission line. This structure also has the capability to inductively tune the isolation optimum value to the different bands and thus can be used in the reconfigurable RF systems. The device shows an insertion loss less than 0.10 dB, a return loss below 36.80 dB up to 25 GHz as compared to 1.00 dB insertion, 7.67 dB return loss for the conventional switch. In the OFF state, proposed device shows two isolation peaks i.e. 48.80 dB at 4.5 GHz and 54.56 dB at 9.7 GHz, when either or both cantilevers are electro-statically actuated to the down-state position respectively. The conventional device has a single isolation peak in the X-band. In addition, improvement of around 3 times in the bandwidth has also been achieved. The designed switch can be used at device and sub-system level for the future multi-band communication applications.

1. Introduction

In recent years, tremendous growth has been seen in the telecommunication sector. New wireless standards are coming-up which require miniaturized devices with large bandwidth, low power consumption and high linearity. The devices with above cited features are also needed to implement the reconfigurable RF front end. This can significantly reduce the number of components, hardware complexity, and cost of the system. RF-MEMS technology has paved the way for the development of such devices. Among the different devices, switches have gained higher attention because of their well known advantages over the solid state counterparts [1–8]. However, switch performance requirement becomes more critical when switches are used in large numbers e.g. multi-port switches, phased array antenna, tunable filters, switch matrix, signal routing and phase shifters etc. [9–12]. Thus, more superior functionality at unit block level becomes essential. A number of structures have been reported in the literature for the capacitive switches having good RF performance in a single band, moderate pull-in voltage, but lags in multi-band functionality [3–6]. The other approach is to combine series and shunt switches to realize multi-band devices. However, higher insertion loss and the large chip area make them unsuitable for future compact systems [13,14].

This work presents a novel capacitive shunt RF-MEMS switch for improving the insertion loss and isolation characteristics. In the proposed device, down-state inductance value can be changed by actuating either or both cantilevers to the down-state. This control over the down-state inductance value cannot be achieved with the conventional capacitive switches [3–6]. This also brings the multi-band functionality as the optimum isolation can be shifted in the different bands. In order to improve the ON state response, the capacitance in the up-state has been reduced by using a float metal layer over the dielectric layer. Further, a comparison of the new design with the equivalent movable bridge switch is also presented. Fig. 1a and b shows the model of the designed switches.

2. Device description and working

In shunt configuration the input and output RF ports are physically connected to each other and therefore normally the switch is ON. The switch is implemented on a 50 Ω CPW line. In the conventional approach, the switch is implemented with a bridge structure. A uniform bridge structure requires higher pull-in voltage so four

* Corresponding author. Tel.: +91 01596 245073, fax: +91 01596 244183.
E-mail address: m.angira@gmail.com (M. Angira).
Peer review under responsibility of Karabuk University.

http://dx.doi.org/10.1016/j.jestch.2015.07.001

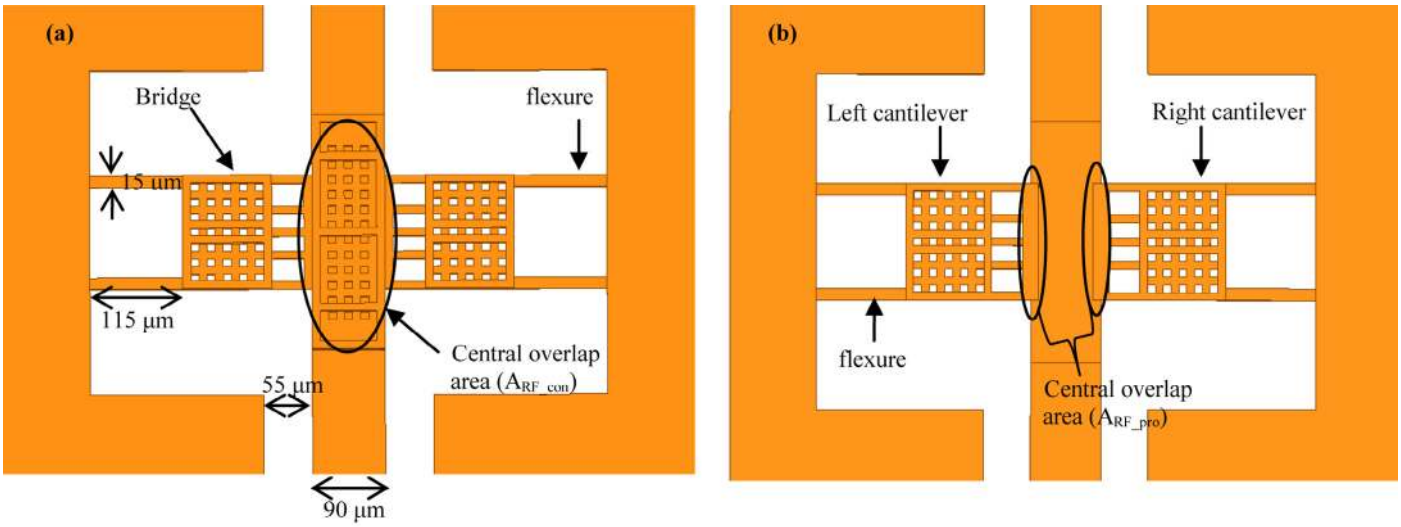

Fig. 1. Top view of the (a) conventional and (b) proposed switches.

flexures attached to a central plate have been chosen to reduce the pull-in voltage. The switch has a central overlap area of $310 \times 90\ \mu m^2$ in order to have maximum isolation in X-band with low insertion loss (<0.2 dB) and pull-in voltage (15 V). In the up-state of switch there is a gap of 2 μm between switch and central conductor of CPW. The actuation electrodes are kept 0.7 μm down from the transmission line in order to alleviate the stiction problem. The proposed switch has been achieved from the bridge based device by disconnecting the central plate. This results in two cantilevers in either side of the transmission line. In order to keep the same down state capacitance in the proposed device, a metal layer has been used over the dielectric layer. In the up-state, the free end of the cantilever has an overlap area of $150 \times 10\ \mu m^2$ with float metal layer. The width of the overlap is limited by the fabrication constraint. As the cantilevers are in parallel, the total overlap area will be $150 \times 20\ \mu m^2$. For actuation, electrostatic method is used as it is compatible with IC technology. The Device dimensions are listed in Table 1.

Table 1
Dimension of the designed switches.

Dimension	Value
Length of bridge and left, right cantilever flexures	115 μm
Width of bridge and left, right cantilever flexures	15 μm
Thickness of all flexures	2 μm
Silicon dioxide thickness (t_{ox})	0.1 μm
Float metal thickness	0.2 μm
Electrostatic gap (d)	2.7 μm
RF gap (g)	2.0 μm
Central overlap area for conventional switch (A_{RF_con})	$310 \times 90\ \mu m^2$
Central overlap area for proposed switch (A_{RF_pro})	$150 \times 20\ \mu m^2$
CPW	55/90/55 μm

2.1. Switch working

The conventional device operates in two states. In the up-state of the bridge, the device shows the insertion loss and down-state corresponds to isolation as depicted in Fig. 2a and b respectively. The proposed switch has four operational states. With both cantilevers in the up position, the signal flows from the input to the output port and the device is ON as shown in Fig. 3a. OFF state can be achieved by actuating either or both cantilevers to down-state as shown in Fig. 3b–d. The device shows two resonant frequencies in the OFF state.

3. Electrical response

For capacitive shunt switch, RF response is the function of the ratio of down-state capacitance to the up-state capacitance. Equations (1)–(3) show the capacitance in up, down and their ratio.

$$C_{up} = \varepsilon_o A_{up}/g \quad (1)$$

$$C_{down} = \varepsilon_o \varepsilon_r A_{down}/t_d \quad (2)$$

$$C_{ratio}(C_{down}/C_{up}) = \varepsilon_r A_{down} g/t_d A_{up} \quad (3)$$

$$C_{up\_Pro}/C_{up\_Con} = 150 \times 20/310 \times 90 \approx 1/9 \quad (4)$$

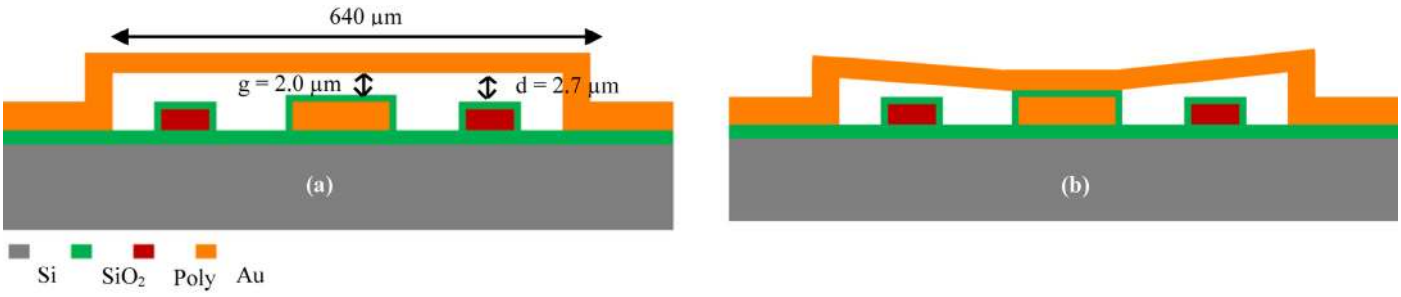

Fig. 2. Cross-sectional view for the working of the conventional switch (a) ON state (b); OFF state.

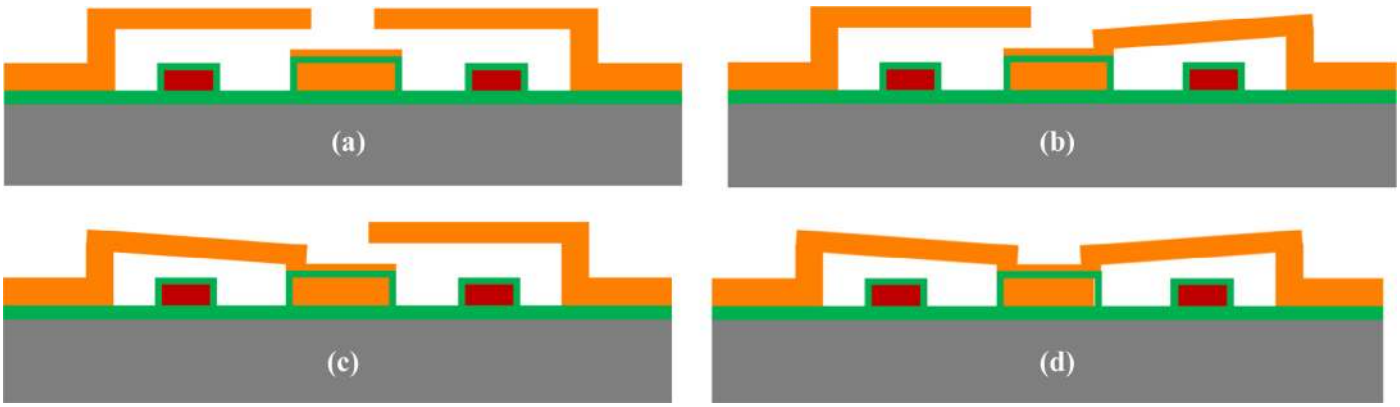

Fig. 3. Cross-sectional view for the working of proposed switch (a) ON state; (b–d) OFF state.

where A_{up} = capacitive overlap area in up-state, A_{down} = capacitive overlap area in down-state, ϵ_o, ϵ_r = free space and relative permittivity respectively, C_{up} = capacitance in the up-state of the switch, C_{down} = down-state capacitance of the switch, C_{ratio} = ratio of the capacitance in down-state to the up-state, and C_{up_Pro}, C_{up_Con} = up state capacitance for proposed and conventional device respectively. A high capacitance ratio is desirable in order to have good insertion loss and isolation response.

3.1. ON state response

In ON state, switch can be modeled as a capacitor in shunt with transmission line. RF response i.e. insertion and return loss during this state can be improved by reducing the $C_{up.}$ The up-state capacitance can be reduced either by decreasing the 'A_{up}' or increasing the 'g'. Any increment in 'g' will increase the pull-in voltage. Alternatively, capacitance in the up-state could be reduced by decreasing the A_{up} but this will change the resonate frequency during OFF state of the device. In the proposed design, this issue has been resolved by utilizing the float metal concept [5,15]. As a metal layer is deposited over the dielectric layer, just the contact is required from the hanging structure to pick up the full capacitance in the down state. Thus, area of overlap between the float metal layer and the hanging structure can be controlled independently. The proposed device has $A_{up\_pro} = 150 \times 20\ \mu m^2$ whereas for bridge structure based $A_{up\_con} = 310 \times 90\ \mu m^2$. Thus, from Eq. (4) C_{up_Pro} is around 9 times less than the C_{up_Con}. In order to investigate the RF performance of both the devices a 3-D structure was created and simulated in Ansys HFSS™. The substrate material is silicon with relative dielectric constant of 11.9 and a 1.3 μm thick SiO_2 layer is used as a buffer layer. The CPW and hanging structure i.e. bridge and cantilevers are assumed to be gold with a conductivity of 4.1×10^7 S/m. Further, a thickness of 0.1 μm of SiO_2 with dielectric constant of 4 has been placed over the central conductor of CPW. The proposed switch shows insertion loss of 0.01–0.10 dB as compared to 0.02–1.00 dB for the conventional device over the frequency range 1 GHz to 25 GHz as shown in Fig. 4a. Return loss is also improved for the novel switch as shown in Fig. 4b.

3.2. OFF state response

In addition to reducing the up-state capacitance, float metal concept also allows to tune the isolation peaks in C and X-bands through cantilever structures by changing the down state inductance. The proposed device has optimum isolation 54.56 dB at 9.8 GHz when both cantilevers are electrostatically actuated to the down state whereas in case of movable bridge device it is observed at 10 GHz as shown in Fig. 5b. The slight disagreement in the OFF state resonant frequency is due to the difference in the down-state capacitances. The capacitance will be less in case of the bridge structure as compared to the proposed device due to the perforation but there would not be much difference in their values due to

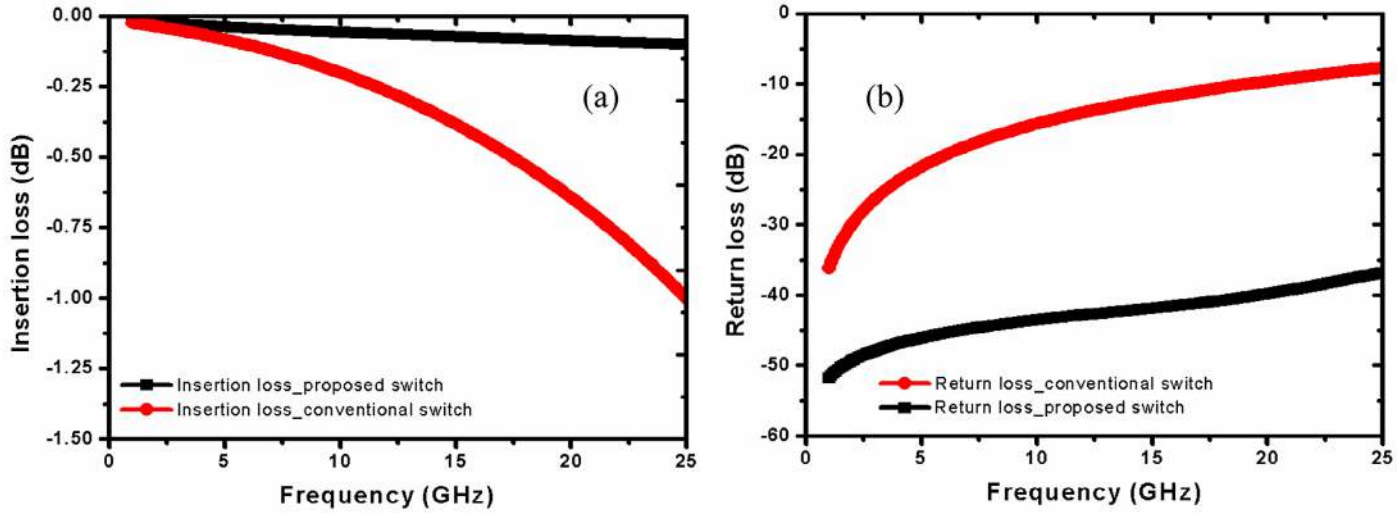

Fig. 4. ON state response of the switches (a) insertion loss; (b) return loss.

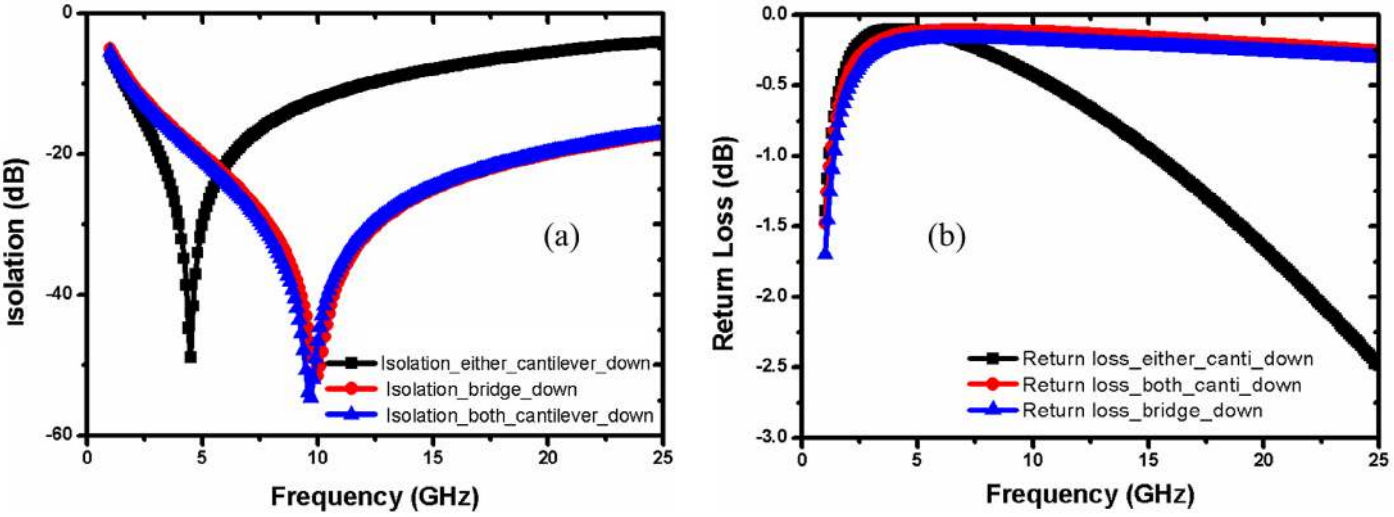

Fig. 5. OFF state response (a) isolation; (b) return loss.

the fringing field effect. Both devices have the identical down state inductance (as the structures in the CPW slot area are the same). As resonant frequency is the function of the down state capacitance and inductance, pulling down either cantilever shifts the optimum isolation to the C-band. A maximum isolation of 48.80 dB at 4.5 GHz has been observed as shown in Fig. 5a. The resonant frequency has been decreased due to the increase in the down state inductance value. Further, the higher inductance value is also responsible for the narrow OFF state response. As the identical cantilevers are used, the OFF-state response will be the same in case either cantilever is actuated to the down state. The Return loss during OFF state for both devices has been shown in Fig. 5b, and is minimum at the resonant frequency.

3.3. Switch bandwidth

The switch bandwidth is calculated from the lower and upper operating frequencies with acceptable maximum insertion loss of 0.2 dB and minimum isolation of 20 dB. The bandwidth for conventional device is 5.0 GHz with $f_L = 5.1$ GHz and $f_U = 10.1$ GHz as shown in Fig. 6a. The lower bound frequency f_L is limited by the minimum isolation, whereas upper operating frequency by the insertion loss. Fig. 6b shows the bandwidth ($f_U - f_L = 15$ GHz) for the proposed device when both cantilevers are in down-state. Bandwidth of 3.2 GHz has been obtained in C-band with either of the cantilever in the down-state as shown in Fig. 7. Thus, in totality, the switch can operate from 3.2 GHz to 19.8 GHz.

In electro-mechanical response, pull-in voltage is determined by doing FEM simulation in coventorware(R). The hanging structure material is gold with Young's modulus of 80 GPa and Poisson's ratio of 0.35. The actuation voltage is applied through the poly-Si electrodes which are placed 115 μm from the anchor location in both devices. The coupled electro-mechanics physics with trajectory as an analysis option and relaxation for iteration method are chosen for extracting the pull-in voltage. The conventional switch has a pull-in voltage of 12.75 V, whereas in the proposed design, cantilevers have a pull-in voltage of 6.0 V as shown in Fig. 8. Further, the cantilevers have been designed to achieve equal pull-in voltage.

4. Effect of residual stress on the proposed device performance

In MEMS technology, thin film movable structures can deform as a result of residual stress. The stress in thin films can be divided into two types: extrinsic, such as stresses arising from the mismatch in thermal expansion coefficients, and intrinsic, such as

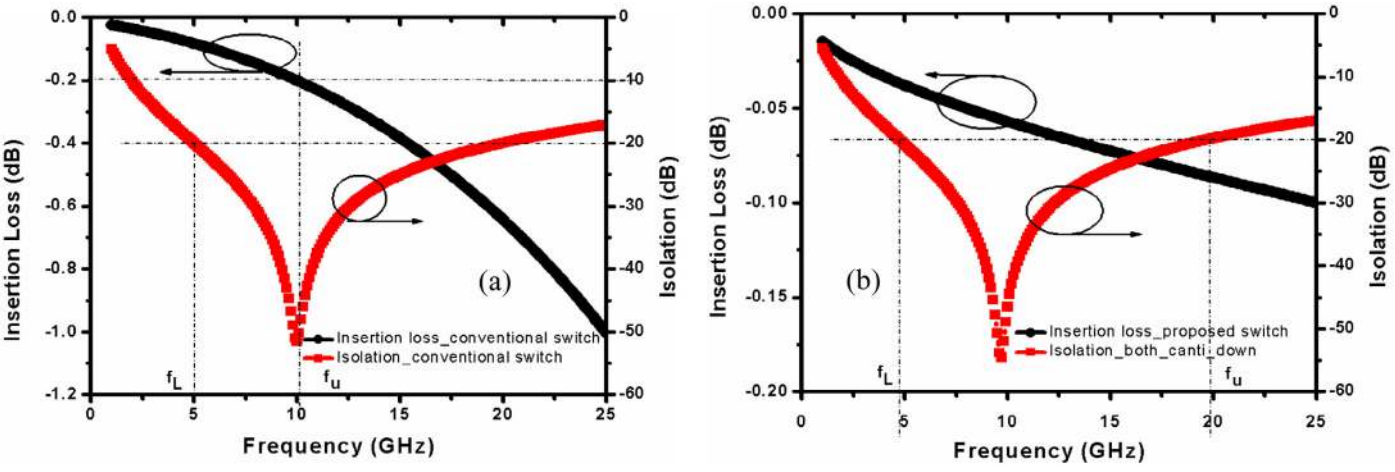

Fig. 6. Bandwidth of the (a) conventional and (b) proposed switches with both cantilevers down.

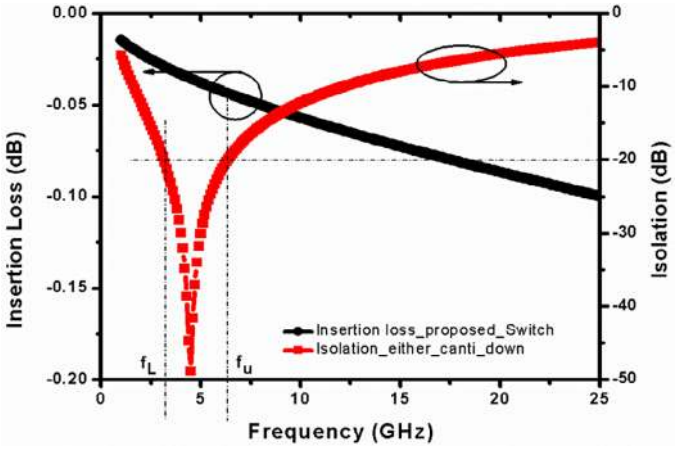

Fig. 7. Bandwidth of proposed device with either of the cantilever to down-state.

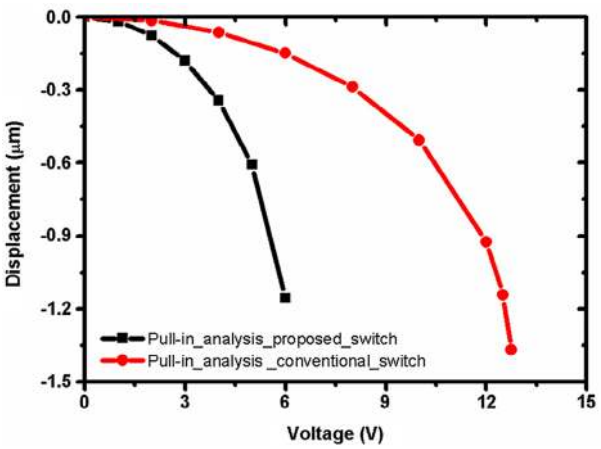

Fig. 8. Pull-in voltage analysis of both switches.

stresses from the nucleation and growth of film deposition. In the first order approximation, general uniaxial residual stress in a thin film can be given by Eq. (5) [16].

$$\sigma_{total} = \sigma_0 + \sigma_1\left(\frac{z}{\frac{h}{2}}\right) \tag{5}$$

where z = coordinate across the thickness (h) with origin chosen at the film's mid plane, σ_0 = mean stress, σ_1 = gradient stress, and σ_{total} = superposition of mean and gradient stress. When a cantilever is released by removing the sacrificial layer, the hanging structure becomes free to deform out-of plane in the form of bending up or down after the relief from gradient stress that existed in the thin film. The mean stress also causes out-of plane deformation in the form of tilt or rotation of the structure due to the in-plane deformation of the portion of the cantilever which is still bonded with the substrate.

4.1. Effect on electromechanical performance

From the previously reported literatures, mean stress and stress gradient were found to vary between 0 MPa to 150 MPa and 0 MPa/μm to 4 MPa/μm respectively for electroplated gold [17–21]. Stress is tensile in nature. The tilt and bending of the beam structure and their effect on the pull-in voltage has been simulated through Coventorware(R) for the range of stress given above. The deformed shape of the cantilever with different mean stress is shown in Fig. 9. A cantilever with more mean stress has a larger normalized air gap, where w_o is the deformation along the length of the cantilever. The cantilever is tilted in the +z direction due the tensile mean stress alone. The maximum tip deflection has been increased from 0.2 μm to 0.41 μm as stress is changed from 50 MPa to 150 MPa. Fig. 9b shows out of plane deflection of cantilever due to the stress gradient acting alone. The cantilever has curled up in the +z direction. The maximum tip deflection has been increased from 0.59 μm to 2.35 μm as stress is changed from 1 MPa/μm to 4 MPa/μm.

Fig. 10a shows the simulated results for cantilever tip deflection as a function of applied voltage subjected to the mean stress. The Pull-in voltage has been increased from 6 V to 8 V as the residual stress value is changed from 0 MPa to 150 MPa. Whereas, pull-in voltage of 10 V has been observed at a stress gradient of 4 MPa/μm as shown in Fig. 10b. In practice, deformations of a cantilever-based structure subjected to mean and gradient stress have both curling and tilt related deformations. Considering the mean

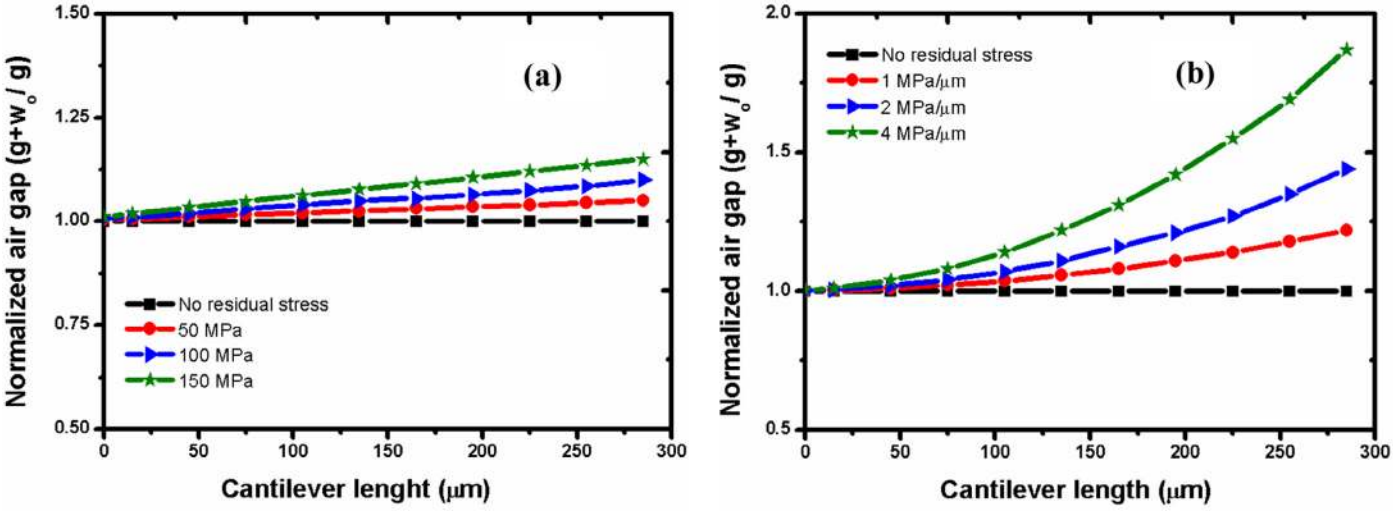

Fig. 9. Deformed shape of cantilever due to (a) mean stress; (b) stress gradients.

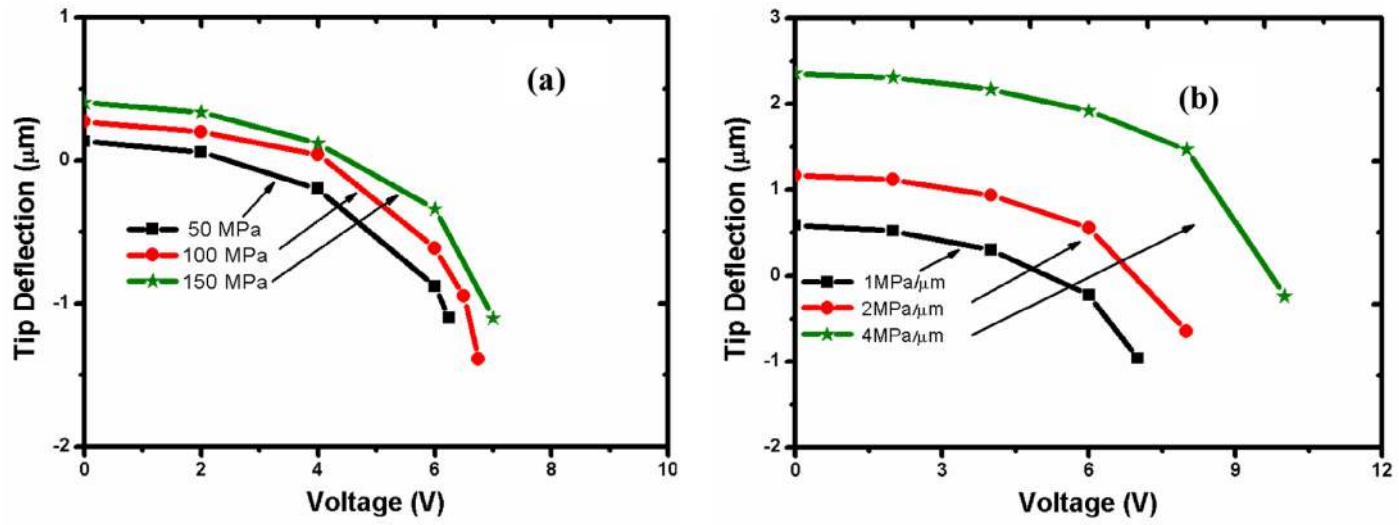

Fig. 10. Pull-in analysis when the cantilever is subjected to (a) mean stress; (b) gradient stress.

stress of 150 MPa and a gradient of 4 MPa/μm, deformation has been simulated for this extreme case as shown in Fig. 11. Further, a pull-in voltage of 11 V has been obtained for this case as shown in Fig. 12.

4.2. *Effect on RF performance*

Residual stress can change the RF response of the switch. During ON state, the response is dependent on the RF overlap area between the hanging structure and the CPW central conductor. As cantilever can deform due to curling and tilting, this will change the up-state capacitance and hence the ON state response. Fig. 13 shows the insertion loss characteristics when the tip of the cantilever is deformed due to the mean and gradient stress. The response with no residual stress case is identical to the cases when the cantilever is subjected to the mean and gradient stress. This is due to the very small capacitor in shunt with the transmission line, which offers high impedance even at a higher frequency. As float metal layer has been used, down-state response will remain the same.

5. Result and discussion

The comparison between the two switches is given in Table 2. The proposed switch has up-state capacitance of 13.50 fF compared to 125.55 fF for the bridge based device. The reduced up-state capacitance improves the ON state response of the device. In OFF state, identical isolation characteristics has been obtained between the proposed switch (with both cantilevers to down-state) and conventional bridge based device. Further, two isolation peaks (C and X-bands) have been achieved due to the effective use of cantilevers in controlling the down-state inductance. The cantilever based switch shows pull-in voltage of 6 V compared to 12.75 V for bridge based switch. The reduction in the pull-in voltage is due to the structural change i.e. from bridge to cantilever and hence the spring constant. Further, the residual stress in the cantilever type structure will increase the pull-in voltage.

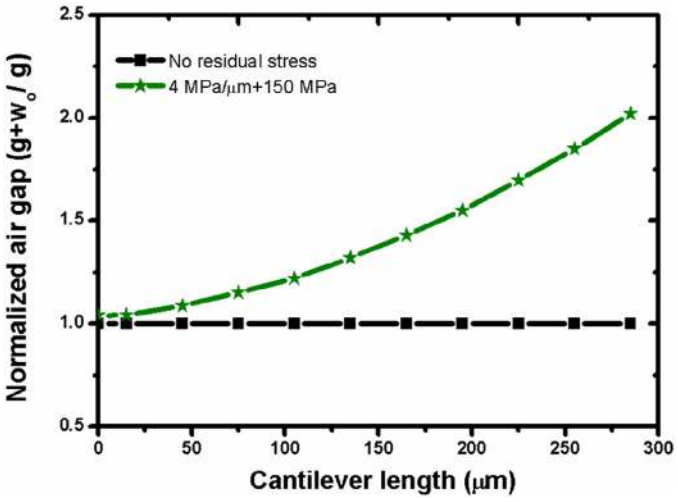

Fig. 11. Deformed shape of cantilever subjected to mean and gradient stress.

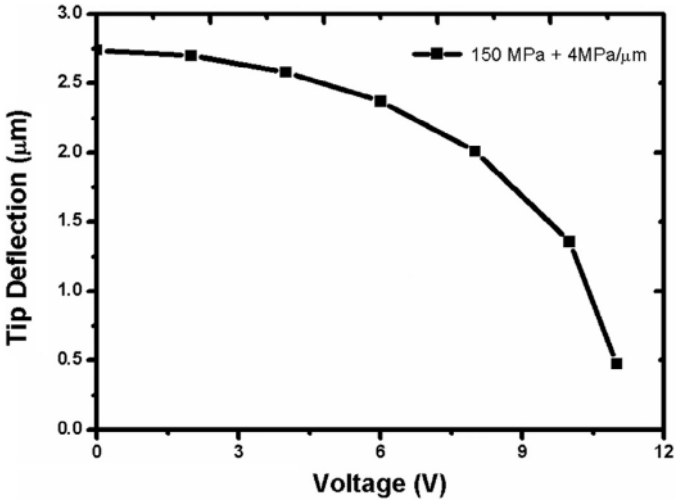

Fig. 12. Pull-in analysis of the cantilever subjected to mean and gradient stress.

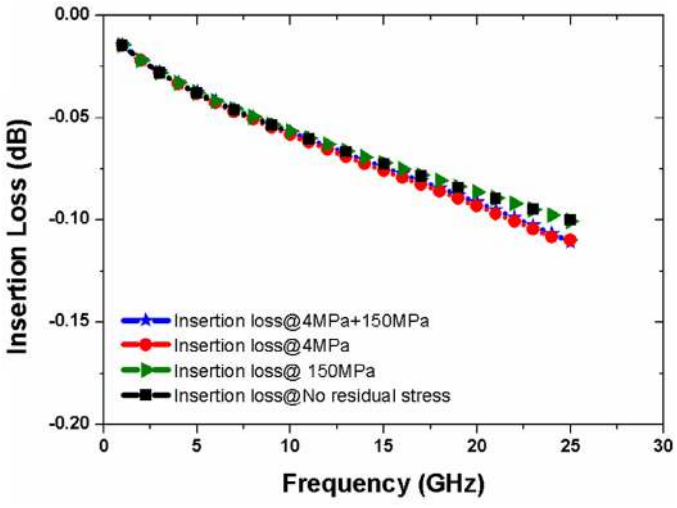

Fig. 13. Comparison of the insertion loss characteristics with cantilever subjected to the residual stress.

6. Conclusion

A new type of capacitive shunt RF-MEMS switch has been investigated. The considerable improvement in insertion loss has been achieved as compared to the conventional switch. In the OFF-state, isolation peaks have been tuned in C and X-bands by varying the down-state inductance through either or both cantilevers. Further, considerable reduction in pull-in voltage and around 3 times improvement in bandwidth has also been observed. The designed switch can be used at device and sub-system levels for the reconfigurable RF front-end.

Table 2
Comparison of the proposed switch with the conventional.

Parameter	Proposed switch	Conventional switch
Up-state capacitance	13.50 fF	125.55 fF
Insertion loss (1–25 GHz)	0.01–0.10 dB	0.02–1.00 dB
Isolation (1–25 GHz)	5.76–3.98 dB (either cantilever to down-state) 5.49–16.94 dB (both cantilever to down state)	5.05–17.10 dB
Isolation peak	2 (C and X-bands)	1 (X-band)
Bandwidth	3.2–19.8 GHz	5.1–10.1 GHz
Pull-in volatge	6.0 V	12.75 V

References

[1] H.A.C. Tilmans, W.D. Raedt, E. Beyne, MEMS for wireless communications from RF-MEMS components to RF-MEMS SiP, J. Micromech. Microeng. 13 (2003) 139–163.
[2] G.M. Rebeiz, RF MEMS Theory, Design and Technology, Wiley, New Jersey, 2003.
[3] K. Rangra, B. Margesin, L. Lorenzelli, F. Giacomozzi, C. Collinni, M. Zen, et al., Symmetric toggle switch – a new type of rf MEMS switch for telecommunication applications: design and fabrication, Sens. Actuators A: Phys 123–124 (2005) 505–514.
[4] M. Angira, K. Rangra, Design and investigation of a low insertion loss, broadband, enhanced self and hold down power RF-MEMS switch, Microsyst. Technol. 21 (2015) 1173–1178.
[5] F. Giacomozzi, C. Calaza, S. Colpo, V. Mulloni, A. Collini, B. Margesini, et al., Development of high con coff ratio RF MEMS shunt switches, Rom. J. Inf. Sci. Tech. (11) (2008) 143–151.
[6] M. Tanga, A.B. Yua, A.Q. Liua, A. Agarwal, S. Aditya, Z.S. Liuc, High isolation X-band MEMS capacitive switches, J. Sensors and Actuators A 120 (2005) 241–248.
[7] K.J. Rangra, Electrostatic low actuation voltage RF MEMS switches for telecommunications (Ph.D. thesis), Department of Information Technology, University of Trento, Trento, 2005.
[8] M. Angira, G.M. Sundaram, K.J. Rangra, A novel interdigitated, inductively tuned, capacitive shunt RF-MEMS switch for X and K bands applications, in: Proceeding of NEMS, Hawaii, USA, 2014, pp. 139–142.
[9] D. Bansal, A. Kumar, A. Sharma, K.J. Rangra, Design of compact and wide bandwidth SPDT with anti-stiction torsional RF MEMS series capacitive switch, Microsyst. Technol. (2014) doi:10.1007/s00542-014-2238-0.
[10] C.J.A. Armenta, S. Porter, A. Marvin, Reconfigurable phased array antennas with RF-MEMS on a PCB substrate, in: Proceeding of antennas and propagation, Loughborough, 1–5, 2012.
[11] D. Peroulis, S. Pacheco, M. Sarabandi, L.P.B. Katehi, MEMS devices for high isolation switching and tunable filtering, in: proceeding of IEEE MTT-S, Boston, 1217–1220, 2000.
[12] S. Dey, S.K. Koul, Design and development of a surface micromachined push–pull-type true-time-delay phase shifter on an alumina substrate for Ka-band T/R module application, J. Micromech. Microeng. 22 (2012) 125006–1250026.
[13] J.B. Muldavin, G.M. Rebeiz, Novel series and shunt MEMS switch geometries for X-band applications, in: Proceeding of European Microwave Conference, Paris, 2000, pp. 1–4.
[14] B. Schauwecker, K.M. Strohm, T. Mack, W. Simon, J.F. Luy, Serial combination of ohmic and capacitive RF MEMS switches for large broadband applications, J. Electron. Lett. 40 (2004) 44–46.
[15] M. Angira, K. Rangra, Performance improvement of RF-MEMS capacitive shunt switch via asymmetric structure design, Microsyst. Technol. 21 (2015) 1447–1452.
[16] W. Fang, J.A. Wickert, Determining mean and gradient residual stresses in thin films using micromachined cantilevers, J. Micromech. Microeng. 6 (1996) 301–309.
[17] A. Sharma, D. Bansal, M. Kaur, P. Kumar, D. Kumar, R. Sharma, et al., Fabrication and analysis of MEMS test structures for residual stress measurement, Sens. & Transducer Journal 13 (2011) 21–30.
[18] T.J. Kang, J.G. Kim, J.S. Lee, J.H. Lee, J.H. Hahn, H.Y. Lee, et al., Low-thermal-budget and selective relaxation of stress gradients in gold micro-cantilever beams using ion implantation, J. Micromech. Microeng. 15 (2005) 2469–2478.
[19] C.D. Patel, G.M. Rebeiz, An RF-MEMS switch with mN contact forces, in: proceeding of IEEE MTT-S, Anaheim, CA, 1242–1245, 2010.
[20] T.J. Kang, J.G. Kim, J.H. Kim, K.C. Hwang, B.W. Lee, C.W. Baek, et al., Deformation characteristics of electroplated MEMS cantilever beams released by plasma ashing, J. Sensors and Actuators A 148 (2008) 407–415.
[21] S.K. Koul, S. Dey, RF MEMS Single-Pole-Multi-Throw Switching Circuits, Springer, India, 2014.